Available online at www.sciencedirect.com
SCIENCE DIRECT®
Thermochimica Acta 414 (2004) 115–120
thermochimica acta
www.elsevier.com/locate/tca

Thermodynamic properties of liquid silver–antimony alloys determined from emf measurements

Agnieszka Krzyżak*, Krzysztof Fitzner

Laboratory of Physical Chemistry and Electrochemistry, Faculty of Non-Ferrous Metals, AGH University of Science and Technology, 30 Mickiewicz Ave., 30-059 Krakow, Poland

Received 12 January 2003; received in revised form 12 January 2003; accepted 12 February 2003

Abstract

The thermodynamic properties of the liquid Ag–Sb alloys were determined using solid oxide galvanic cells with zirconia electrolyte. The emfs of the cells:

$Ag_xSb_{(1-x),}Sb_2O_3/O^{2-}/air$

were measured in the temperatures range 950–1100 K in the whole range of the alloy compositions.

First, the Gibbs free energy of formation of liquid Sb_2O_3 from pure elements was derived:

$\Delta G^{\circ}_{f(Sb_2O_3)}$ (J/mol) $= -687100 + 243.23T$.

Next, the activities of antimony were measured as a function of the alloy compositions, x. Redlich–Kister polynomial expansion was used to describe the thermodynamic properties of the liquid phase. From the model equations the limiting value of the logarithm of activity coefficient of antimony in silver was obtained as a function of temperature:

$\ln \gamma^0_{Sb} = -3812.5/T + 0.4112.$

The obtained results were compared with the experimental values reported in the literature.

Keywords: Sliver alloy; Solid electrolyte; Thermodynamics; emf measurement

1. Introduction

The process of silver production from sledges left after copper electrochemical refining is based in principle on the subsequent reduction and oxidation stages carried out in Kaldo furnace. The resulting distribution of solutes between silver and the slag phases is dependent on both: temperature and oxygen partial pressure applied during the process. Thus, thermodynamic properties of silver multicomponent alloy must be known first before any attempt to predict alloying elements distribution is undertaken. Moreover, before this kind of analysis is attempted for the multicomponent alloy, the thermodynamic properties of all binaries being respective parts of this multicomponent solution should be known exactly.

Consequently, since antimony is one of the solutes being present in silver, the knowledge of its activity, especially in dilute solution range, is required to predict its behavior during the reaction with the slag phase.

The thermodynamic properties of the liquid silver–antimony alloys were examined by different research groups. They used various experimental techniques but, surprisingly, there are only a few data on Sb activity in these alloys. The integral heat of mixing was measured by Castanet et al. [1] at 950, 1100 and 1300 K. These results indicate temperature dependence of the heat of mixing. Predel and Emam [2] measured the heat of mixing at 1250 K and these results are almost identical with those of Castanet et al. obtained at 1300 K.

* Corresponding author. Tel.: +48-126174124; fax: +48-1263323.
E-mail address: akrzyzak@uci.agh.edu.pl (A. Krzyżak).

0040-6031/$ – see front matter © 2003 Elsevier B.V. All rights reserved.
doi:10.1016/j.tca.2003.12.005

The activity of antimony in the alloy was determined by Hino et al. [3] who measured vapor pressure of antimony using the transportation method between 1273 and 1473 K. In turn, Nozaki et al. [4] and Vecher and Gerasimov [5] employed galvanic cells with molten salts electrolyte and solid silver reference electrode. From the measured emfs, the activity of silver as well as its partial thermodynamic functions were determined. In the present work we employed galvanic cells with the solid oxide electrolyte for the determination of Sb activity in the liquid Ag–Sb alloys.

2. Experimental

2.1. Materials

Metallic silver was obtained from POCh, Gliwice, while antimony was obtained from Fluka AG, Buchs SG, Switzerland. They were 99.99 and 99.999% pure, respectively. Antimony oxide, Sb_2O_3, was obtained from POCh, Gliwice and was 99.9% pure. Closed at one end yttria stabilized zirconia solid electrolyte tubes (length 50 mm, outside diameter 8 mm) were supplied by the Friatec DG, Germany. Antimony–silver alloys were prepared from pure metals separately by melting weighed pure metals in evacuated and sealed silica capsules.

2.2. Technique

The experimental technique is in principle similar to that used by us in the previous study of Ag–Bi alloys [6], though the cell construction is different. A schematic representation of the cell assembly is shown in Fig. 1. The tube of solid zirconia electrolyte contained about 2 g of metallic alloy of a chosen composition. Alloys of Ag–Sb were prepared separately from pure metals by melting weighed amounts of antimony and silver in the silica capsules evacuated and sealed under vacuum. The kanthal wire with welded Re wire tip, kept inside the alumina shield, acted as an electric contact with a liquid metal electrode. The platinum wire was connected to the outer part of the electrolyte tube and worked as an air reference electrode. The whole cell was placed inside the silica tube, which was suspended on an upper brass head, which closed the tube of a resistant furnace. The cell was kept in the constant temperature zone of the furnace under a stream of purified argon. The temperature inside the cell was maintained constant within ±1 K.

After the required cell temperature was reached first time, the cell was left overnight to attain equilibrium. The emf of the cell was then recorded by means of the digital multimeter Keithley 2000 (USA) and next the temperature was changed. The measurements were carried out at increasing and decreasing temperature for several days.

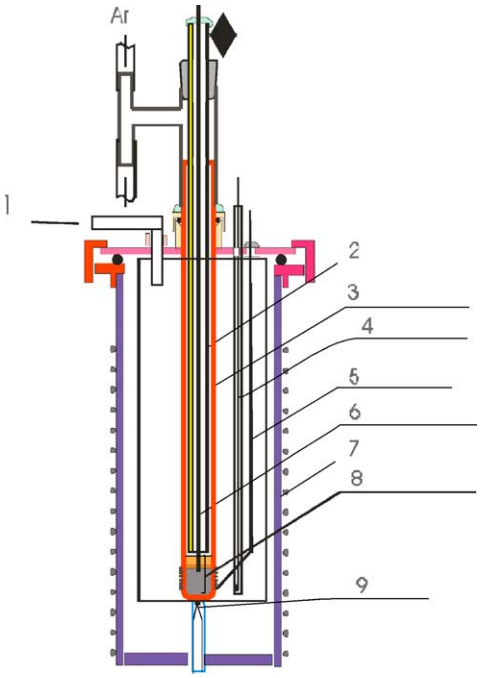

Fig. 1. Galvanic cell assembly: 1, air; 2, alumina shield; 3, solid electrolyte; 4, thermocouple; 5, wire Pt; 6, kanthal + *Re*; 7, resistant furnace; 8, working electrode; 9, thermocouple.

3. Results

In order to determine the antimony activity in liquid Ag–Sb alloys the emf of the cell I

$$\mathrm{Re} + \text{kanthal}, \mathrm{Ag}_x\mathrm{Sb}_{(1-x)}, \mathrm{Sb_2O_{3(l)}}/\mathrm{O^{2-}}/\text{air}, \mathrm{Pt} \quad \text{(I)}$$

was measured in the temperature range 950–1100 K. The cell scheme is written in such a way that the right-hand electrode is positive. For galvanic cell I the electrode reactions are:

(a) at the RHS electrode:

$$\tfrac{3}{2}\mathrm{O_2} + 6\mathrm{e} \leftrightarrow 3\mathrm{O^{2-}} \quad (1)$$

(b) at the LHS electrode:

$$2\mathrm{Sb} + 3\mathrm{O^{2-}} \leftrightarrow \mathrm{Sb_2O_3} + 6\mathrm{e} \quad (2)$$

Consequently, the overall cell I reaction is:

$$\tfrac{3}{2}\mathrm{O_2} + 2\mathrm{Sb} \leftrightarrow \mathrm{Sb_2O_3} \quad (3)$$

For the reversible reaction (3) the change in Gibbs free energy can be derived as follows:

$$\Delta G = -6\mathrm{FE} = \mu_{\mathrm{Sb_2O_3}} - 2\mu_{\mathrm{Sb}} - \tfrac{3}{2}\mu_{\mathrm{O_2}} = \Delta G^\circ - 2RT\ln a_{\mathrm{Sb}} - \tfrac{3}{2}RT\ln p_{\mathrm{O_2}} \quad (4)$$

If antimony is in its pure, liquid state ($a_{\mathrm{Sb}} = 1.0$) Eq. (4) takes the form:

$$-6\mathrm{FE}^\circ = \Delta G^\circ_{\mathrm{f(Sb_2O_3)}} - \tfrac{3}{2}RT\ln p_{\mathrm{O_2}} \quad (5)$$

where $p_{\mathrm{O_2}}$ denotes the oxygen partial pressure of the air reference electrode. Then, from Eq. (5) the Gibbs free energy

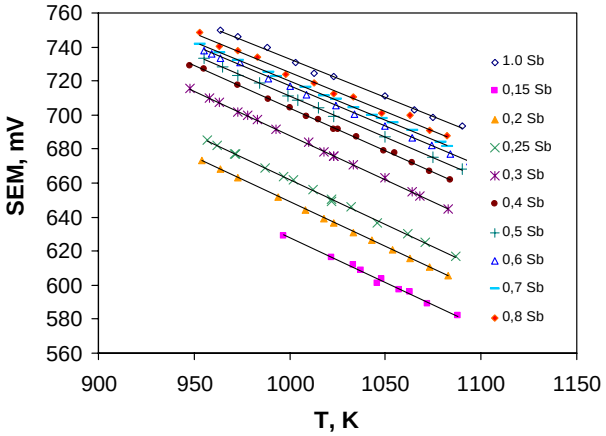

Fig. 2. Temperature dependence of the emf of liquid Sb_2O_3.

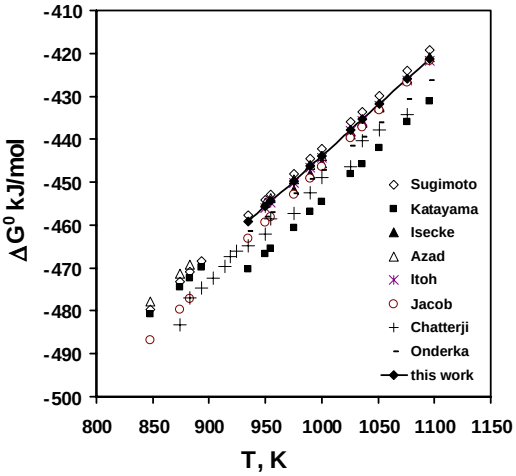

Fig. 3. Gibbs free energy of formation of the liquid Sb_2O_3.

of formation of the liquid Sb_2O_3, $\Delta G^{\circ}_{f(Sb_2O_3)}$, can be determined from E^0 measured against the air reference electrode as a function of temperature.

emf values produced by the cell I in the range of temperature from 950 to 1100 K after the necessary thermo-emf Pt-Kanthal + Re corrections are shown in Fig. 2. The resulting linear equations obtained by the least square method, are presented in Table 1.

At first, from the results obtained for the equilibrium between pure liquid antimony and liquid antimony oxide, the Gibbs free energy change for the reaction of formation of Sb_2O_3 was derived using Eq. (5). The obtained values of Gibbs free energy yield the following temperature dependence:

$$\Delta G^{\circ}_{f(Sb_2O_3)}\,(\mathrm{J/mol}) = -687100 + 243.23T \tag{6}$$

Our data, represented by Eq. (6), are shown in Fig. 3 and compared with the results of other electrochemical high temperature studies [7–14]. A good agreement is found between all studies with the spread of the data of the order of 15 kJ, which is about 3.5% of the measured value.

Next, by combining Eqs. (4) and (5) the following expression for the activity of antimony in the alloy with silver can be derived:

$$\ln a_{Sb} = \left(\frac{3F}{RT}\right)(E - E^0) \tag{7}$$

where F is the Faraday constant, T the absolute temperature, and R the gas constant.

From the measured emfs the expression for the partial Gibbs free energy of antimony in the alloy can be derived

$$\Delta\bar{\mu}_{Sb} = 3F(E - E^0) = 3F(\Delta a + \Delta bT) \tag{8}$$

if the linear dependence of the type $a + bT$ is assumed for temperature variation of the emf

Then, using the well known relationship, the partial entropy of antimony can be defined as

$$\Delta\bar{S}_{Sb} = -\left(\frac{\partial\,\Delta\bar{\mu}_{Sb}}{\partial T}\right)_p = -3F\,\Delta b \tag{9}$$

as well as the partial enthalpy:

$$\Delta\bar{H}_{Sb} = (\Delta\bar{\mu}_{Sb} + T\,\Delta\bar{S}_{Sb}) = 3F\,\Delta a \tag{10}$$

Thus, having experimentally determined E versus T plots for alloys of different composition, all partial thermodynamic functions of antimony in the alloy can be derived.

The activities of antimony in the alloy were calculated at 1073 K from the emf values and are plotted in Fig. 4. The standard state of antimony is pure liquid Sb. Eq. (7) was used to calculate activities for the respective alloy compositions from the data gathered in Table 1.

Before an attempt to describe the thermodynamic properties of the liquid solutions analytically was made, the activity coefficient of antimony at infinite dilution with silver was derived. According to Darken [15] the whole concentration range of the investigated system can be divided into terminal regions if $\ln\gamma_2$ versus $(1 - X_2)^2$ is plotted at a constant temperature. This so-called α-function method yields linear dependence of $\ln\gamma_2$ in the limit $X_2 \geq 0$ and consequently $\ln\gamma^0$ at infinite dilution can easily be obtained. In Fig. 5 this

Table 1
The temperature dependence of the emf of cell I

X_{Sb}	E (mV) $= a + bT$ (K)	σ
0.80	1191.7–0.4669T	±4.45
0.70	1178.6–0.4588T	±0.25
0.60	1189.1–0.4721T	±0.53
0.50	1191.1–0.4803T	±0.52
0.40	1203.4–0.4994T	±0.55
0.30	1209.3–0.5210T	±0.46
0.25	1187.1–0.5249T	±0.66
0.20	1173.9–0.5250T	±0.31
0.15	1150.3–0.5225T	±1.77
1.00	1186.7–0.4537T	±1.08

σ is a standard deviation of E.

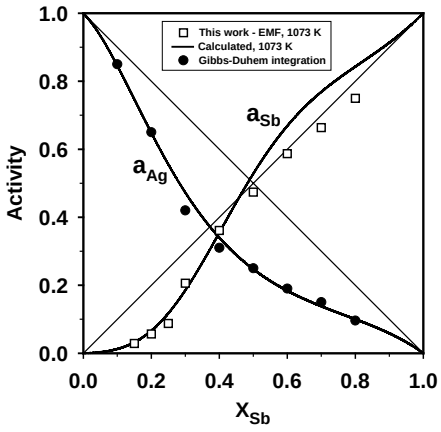

Fig. 4. Activities of components in Ag–Sb liquid alloys at $T = 1073$ K.

Darken's plot is shown for $\ln \gamma_{Sb}$ at 1073 K. The limiting value obtained in this way is equal to $\ln \gamma^0_{Sb} = -3.133$.

Having the limiting value of $\ln \gamma^0_{Sb}$ at 1073 K, one can integrate Gibbs–Duhem equation to obtain $\ln \gamma_{Ag} = f(X_{Sb})$ at the same temperature. Using well-known relationship

$$\mathrm{d} \ln \gamma_{Ag} = -\int_{X_{Sb}=0}^{X_{Sb}} \left(\frac{X_{Sb}}{X_{Ag}} \right) \mathrm{d} \ln \gamma_{Sb} \tag{11}$$

logarithms of the activity coefficient of silver were calculated and are shown together with values determined from emfs. The $\ln \gamma$ versus composition plots obtained in this way are shown in Fig. 6. Also, the activities of silver were calculated and are shown in Fig. 4.

In principle, all partial functions can be obtained in this way for both components. However, since the split of the partial Gibbs free energy between enthalpy and entropy terms is always uncertain in electrochemical studies, we followed different approach. It is based on computer optimization of thermodynamic data existing for a given phase.

We selected the integral heat of mixing data from the literature. Calorimetric data of Predel and Emam [2] at 1250 K, and Castanet et al. [1] at the highest experimental temperature 1300 K were chosen and they are shown in Fig. 7. We also accepted antimony activities calculated at 1073 K from

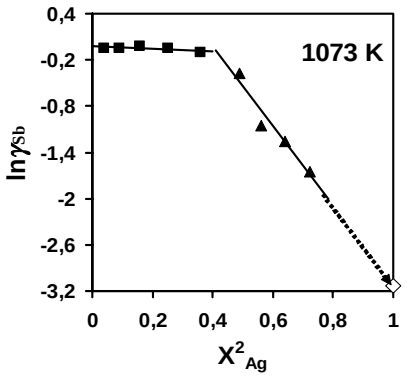

Fig. 5. Relation between $\ln \gamma_{Sb}$ and $(1 - x_{Ag})^2$ at 1073 K.

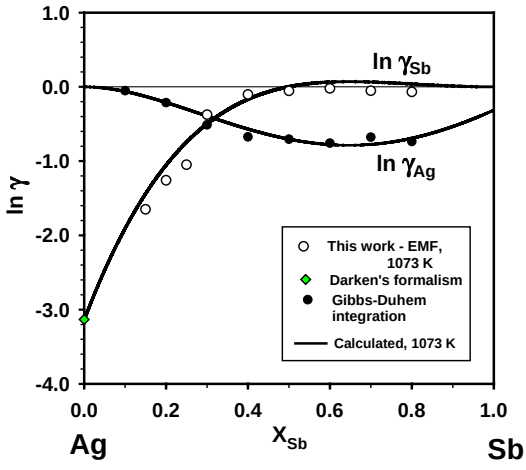

Fig. 6. Composition dependence of $\ln \gamma$ for both components at 1073 K.

our own emf measurements together with limiting values of $\ln \gamma^0_{Sb}$ obtained with α-function method. These data were used together to describe the thermodynamic properties of the liquid phase.

The results were described with the Redlich and Kister formula [16]. It is assumed that the liquid solution phase is described by the disordered substitutional solution model and its excess Gibbs energy is expressed by the following equation:

$$\Delta G^E = X_{Sb}(1 - X_{Sb})[L^0_{Ag,Sb} + (1 - 2X_{Sb})L^1_{Ag,Sb} + (1 - 2X_{Sb})^2 L^2_{Ag,Sb} + \dots] \tag{12}$$

in which X_{Sb} is the mole fraction of antimony.

The expression of the partial excess Gibbs free energy of antimony resulting from this model is:

$$\Delta G^E_{Sb} = (1 - X_{Sb})^2[L^0_{Ag,Sb} + (1 - 4X_{Sb})L^1_{Ag,Sb} + (1 - 2X_{Sb})(1 - 6X_{Sb})L^2_{Ag,Sb} + \dots] \tag{13}$$

Consequently, from these equations all thermodynamic functions in the solution can be determined. Parameters

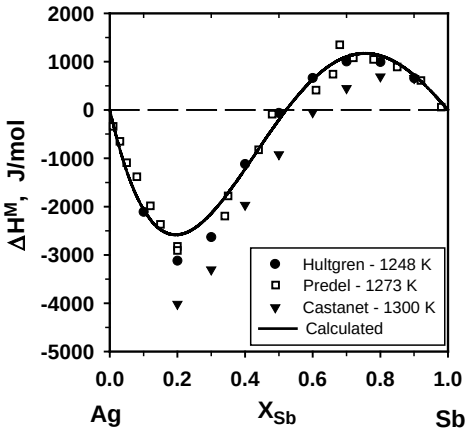

Fig. 7. Enthalpy of mixing in the liquid Ag–Sb system.

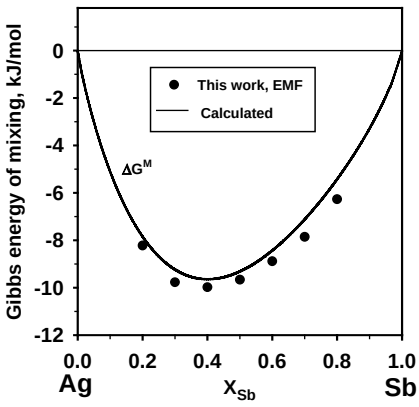

Fig. 8. Integral Gibbs energy of mixing in the liquid Ag–Sb system at 1073 K.

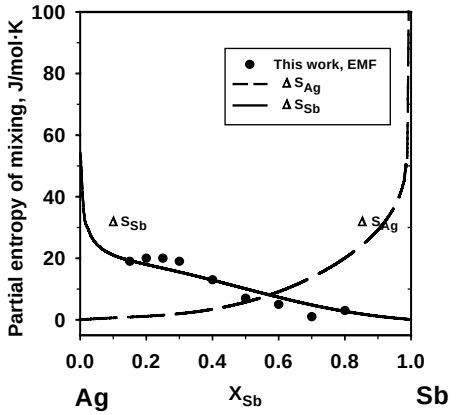

Fig. 10. Partial entropy of components in the liquid Ag–Sb system.

$L^{i}_{\mathrm{Ag,Sb}}$ are linearly dependent on temperature and are given in J/mol. Their values resulting from our calculations are as follows:

$$L^{0}_{\mathrm{Ag,Sb}} = -3619.5 - 8.2962T$$
$$L^{1}_{\mathrm{Ag,Sb}} = -21732.2 + 8.4996T \quad (14)$$
$$L^{2}_{\mathrm{Ag,Sb}} = -6345.2 + 3.2151T$$

Figs. 4 and 7 show comparison of the activities of antimony and silver derived from experiments, and the heat of mixing of the Ag–Sb alloy, with the results of model calculations. Integral Gibbs energies of solutions calculated from obtained activities are compared in Fig. 8 with those calculated from the model. The determined partial enthalpy and partial entropy functions in the liquid Ag–Sb system are shown in Figs. 9 and 10, and are also compared with the results of calculations. The experimental values were calculated from respective coefficients of linear dependencies given in Table 1 and using expressions (9) and (10). Model calculations were performed with Redlich–Kister formula. A good agreement is found between calculated and measured values.

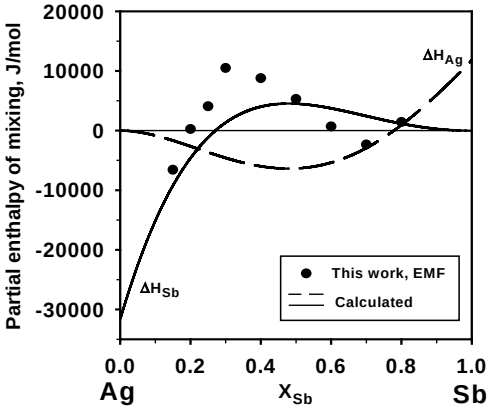

Fig. 9. Partial enthalpy of components in the liquid Ag–Sb system.

Our measurements were performed in the temperature range 950–1100 K and over the whole concentration range of the alloy. Increasing discrepancy between calculated and measured values of activities (visible for Sb-rich solutions) probably results from growing uncertainty of these values as the difference $(E - E^{0})$ in Eq. (7) decreases for $X_{\mathrm{Sb}} \geq 1.0$.

The positive (for $X_{\mathrm{Sb}} \to 1.0$) and negative (for $X_{\mathrm{Sb}} \to 0$) deviations from the Raoult's Law obtained from the model's calculations are not so surprising. This kind of deviation is indicated by the measured heat of mixing (Fig. 7). Moreover, diffraction experiments on Cu–Sb liquid alloys done by means of neutron diffraction and X-rays by Knoll and Steeb [17] at temperatures about 10° above liquidus indicate not only the clustering of atoms in the liquid but also segregation tendency. The simultaneous existence of compound regions and segregation regions within the melt depending on the concentration must influence the sign of the deviation of activities from the Raoult's Law. Since the Ag–Sb phase diagram is very similar to that of Cu–Sb system [18] one may expect that similar phenomenon takes place in the Ag–Sb liquid solution.

Since we are mainly interested in the antimony behavior in silver at low antimony concentration range, the logarithm of the activity coefficients of antimony was derived for $X_{\mathrm{Sb}} \geq 0$ from Redlich–Kister formula (13) obtained after optimization. It is given by the following temperature dependence:

$$\ln \gamma^{0}_{\mathrm{Sb}} = -\frac{3812.5}{T} + 0.4112 \quad (15)$$

Our measurements were carried out at temperatures lower than those of the industrial process we are interested in. Thus, in order to check the obtained temperature dependence, we compared our calculated values with the experimental results of Hino et al. [3]. It is the only experimental study we found in the literature in which the activity of antimony was determined by vapour pressure measurements at temperature as high as 1473 K. Fig. 11 shows the comparison of experimental and calculated values for $\ln \gamma_{\mathrm{Sb}}$ at this temperature. This comparison suggests that in the dilute

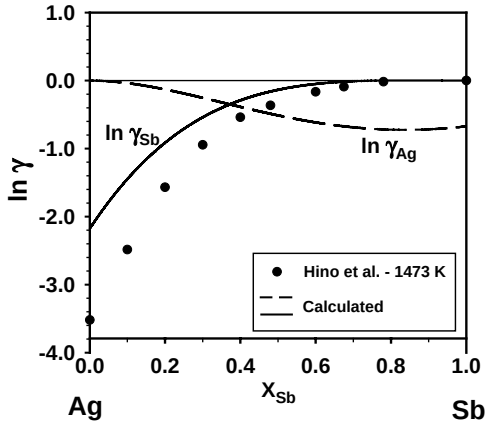

Fig. 11. Ln γ vs. composition plot at 1473 K.

solution range and temperature of the industrial process, the value of γ^0_{Sb} may be higher than the results of Hino et al. suggest.

4. Conclusions

It was demonstrated that properly designed electrochemical cell with zirconia solid electrolyte can provide reliable thermodynamic information about the liquid Ag–Sb solutions. The comparison of the Gibbs free energy of formation of the liquid Sb_2O_3 obtained in this study with the literature data speaks for reliability of our electrochemical cell performance. Full thermodynamic description of the liquid phase is given. Redlich–Kister formula was used to describe temperature and composition dependence of thermodynamic functions. Our results indicate that at temperature of 1473 K limiting value of $\ln \gamma_{Sb}$ in silver obtained from calculations is higher than that resulting from the study of Hino et al.

Acknowledgements

This work was supported by the State Committee for Scientific Research under Grant No. 7TO8B05120.

References

[1] C. Castanet, Y. Claire, M. Gilbert, G. Laffitte, Rev. Hautes Temper. Refract 7 (1970) 51.
[2] B. Predel, A. Emam, Z. Metallkd. 64 (1973) 496.
[3] M. Hino, T. Azakami, M. Kameda, J. Jpn. Int. Metals 39 (1975) 1175.
[4] T. Nozaki, M. Shimoji, K. Niwa, Ber. Bunsenges. 70 (1966) 207.
[5] A.A. Vecher, Y.I. Gerasimov, Doklady Acad. Sci. URSS 139 (1961) 863.
[6] W. Gąsior, J. Pstruś, Z. Moser, A. Krzyżak, K. Fitzner, J. Phase. Equil. 24 (2003) 40.
[7] E. Sugimoto, S. Kuwata, Z. Kozuka, J. Jpn. Inst. Metals 44 (1980) 644.
[8] I. Katayama, J. Shibata, Z. Kozuka, J. Jpn. Inst. Metals 39 (1975) 990.
[9] B. Isecke, PhD Thesis, Tech. Univ., Berlin, 1977.
[10] A.M. Azad, R. Pankajavalli, O.M. Sreedharan, J. Chem. Thermodyn. 18 (1986) 255.
[11] S. Itoh, T. Azakami, J. Jpn. Inst. Metals 48 (1984) 293.
[12] K.T. Jacob, P.M. Mathew, Z. Metallkde. 70 (1979) 366.
[13] D. Chatterji, J.V. Smith, J. Electrochem. Soc. 120 (1973) 889.
[14] B. Onderka, J. Wypartowicz, K. Fitzner, Thermochim. Acta 260 (1995) 29.
[15] L.S. Darken, Trans. Met. Soc. AIME 239 (1967) 80.
[16] O. Redlich, A.T. Kister, Ind. Eng. Chem. 40 (1948) 345.
[17] W. Knoll, S. Steeb, Phys. Chem. Liquids 4 (1973) 39.
[18] T.B. Massalski (Ed.), Binary Alloys Phase Diagrams, vols. 1–3, 2nd ed., ASM International, Materials Park, OH, 1990.